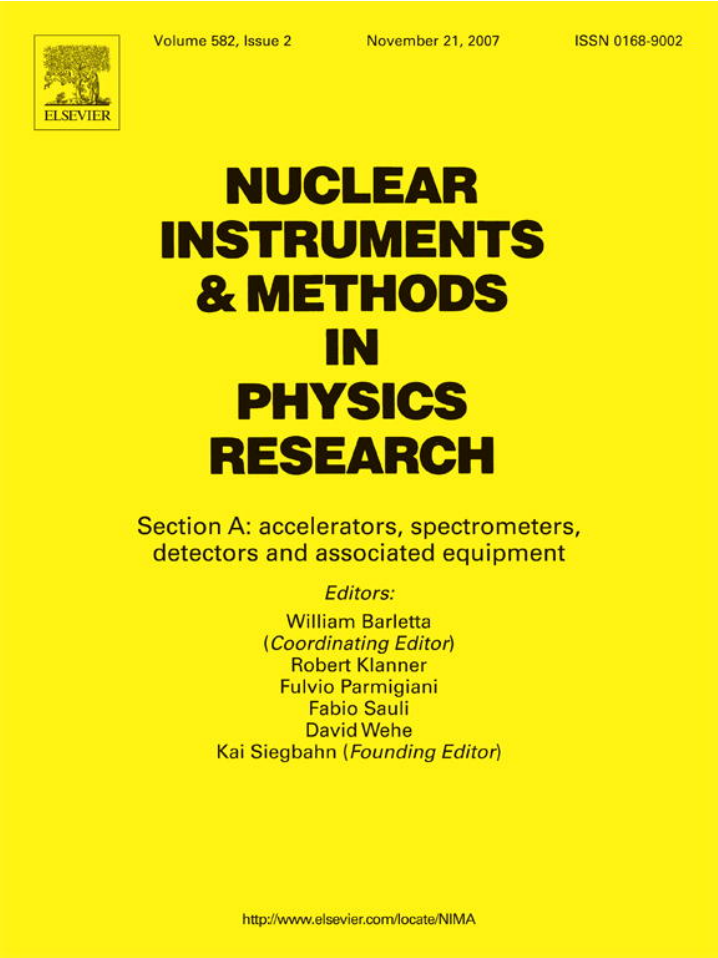

Volume 582, Issue 2 November 21, 2007 ISSN 0168-9002

NUCLEAR
INSTRUMENTS
& METHODS
IN
PHYSICS
RESEARCH

Section A: accelerators, spectrometers,
detectors and associated equipment

http://www.elsevier.com/locate/NIMA

Available online at www.sciencedirect.com
ScienceDirect
ELSEVIER
Nuclear Instruments and Methods in Physics Research A 582 (2007) 554–561
NUCLEAR INSTRUMENTS & METHODS IN PHYSICS RESEARCH Section A
www.elsevier.com/locate/nima

Investigation of the properties of a 1″ × 1″ LaBr$_3$:Ce scintillator

R. Nicolini, F. Camera*, N. Blasi, S. Brambilla, R. Bassini, C. Boiano, A. Bracco, F.C.L. Crespi, O. Wieland, G. Benzoni, S. Leoni, B. Million, D. Montanari, A. Zalite[1]

University di Milano and INFN sez. of Milano, Via Celoria 16, 20133 Milano, Italy

Received 20 February 2007; received in revised form 2 August 2007; accepted 4 August 2007
Available online 31 August 2007

Abstract

The properties of a cylindrical 1″ × 1″ LaBr$_3$:Ce scintillator (Brillance 380) were investigated. The energy resolution at γ-ray energy of 662 keV was measured to be smaller than 3% and the intrinsic time resolution was found to be $\approx$230 ps. Two different aspects were investigated. The first is the detailed study of the crystal self-activity, emitting α and β particles and γ-rays, by measuring coincidences with γ-rays in HPGe, BGO and BaF$_2$ detectors. In particular, the coincidence with an HPGe detector allowed to isolate clearly the different contributions from ^{227}Ac (chemical homologue of lanthanum) and its daughter nuclei down to the stable ^{207}Pb. The second aspect is the determination of the efficiency for γ-ray detection, measured at 1 MeV and simulated using GEANT4 up to 15 MeV as a function of the detector size.

PACS: 95.55.Ka; 24.10.Lx; 29.40.Mc

Keywords: LaBr$_3$ scintillators; Lanthanum halide; Gamma spectroscopy; Gamma detectors; Self-activity; Simulations

1. Introduction

Presently, LaBr$_3$:Ce scintillators are attracting particular interest for γ-spectroscopy measurements due to their good time resolution (of the order of few hundreds picoseconds) and energy resolution ($<$3% at 662 keV), the latter being the best obtainable with scintillators. In addition, due to the high Z of lanthanum and high density of the crystal, these detectors, if made with large volumes, are of potential use for high-energy γ-rays (up to 20 MeV). The general properties of LaBr$_3$:Ce are described in Refs. [1–7] together with comparisons with the other scintillators typically employed in gamma spectroscopy.

The LaBr$_3$:Ce detectors with their good performances could become an interesting alternative to HPGe detectors in γ spectroscopy in situations in which the measured spectra are not very complex or in which the Doppler broadening due to the velocity of the emitting source is larger than the intrinsic resolution of the HPGe and comparable to that of LaBr$_3$:Ce. This could be the case of specific in-beam measurements with fast exotic beams. In addition, the excellent timing properties allow to measure the time of flight with high resolution, information usually used for neutron–γ discrimination and for background rejection. However, a good use of LaBr$_3$:Ce detectors requires an accurate determination of the self-activity, particularly when low background is required or when events are collected at extremely low trigger rates (few events per hour). In fact, spurious peaks due to internal activity might affect the identification and the measurement of the peaks of interest. Both, the background rejection by time of flight and the accurate knowledge of the internal activity of the detectors, are especially crucial in the spectroscopy with radioactive beams (see, e.g. the discussion on background radiation in Ref. [8]). On the other hand, if the internal activity rate is negligible compared to the event rate and/or can be eliminated with the experiment trigger conditions, it can be used as an intrinsic calibration source useful to monitor gain drifts.

---

*Corresponding author.
E-mail address: camera@mi.infn.it (F. Camera).

[1] Present address: Petersburg Nuclear Physics Institute, Gatchina, St. Petersburg, Russia.

doi:10.1016/j.nima.2007.08.221

This is an essential point in the measurement of continuum spectra (see, e.g. Refs. [9–11]). The approach of using the internal activity of the detector has been extensively used in measurements of the γ decay from the giant dipole resonance in hot rotating nuclei with BaF_2 detectors. Therefore, an accurate investigation of the properties of $LaBr_3$:Ce crystal is important also in this connection.

In the past years (when $LaBr_3$:Ce was not commercially available) few very accurate studies of the self-activity in $LaCl_3$:Ce [12–15], very similar to that of $LaBr_3$:Ce, were made. It was found that in $LaCl_3$:Ce crystals the self-activity is due by two sources: the presence of the unstable ^{138}La isotope and a contamination with the element ^{227}Ac, being the lanthanum chemical homologue. Presently, there is only one work in literature focusing on the problem of the self-activity in $LaBr_3$:Ce [16], although the problem was raised also in other papers (see for example Ref. [5]). In the work of Ref. [16], the self-activity was studied for a 1″ × 1″ $LaCl_3$ crystal and for a smaller $LaBr_3$:Ce crystal (0.5 g) in a low-background counting chamber setup. However, only signals "in singles" were recorded for the $LaBr_3$:Ce crystal, and no coincidence or anticoincidence measurements with other detectors were made. It should be noted that coincidence measurements are indeed very useful to isolate the different contributions of the internal activity.

Another property of these detectors to be investigated is the efficiency at different γ-ray energies, information that will be useful in view of their potential use in nuclear structure studies through in-beam γ-ray spectroscopy involving γ-ray energies ranging from 100 keV to 15–20 MeV. For this, in addition to the measurements with the available $LaBr_3$:Ce detectors, it is useful to perform simulations of the detector response to deduce the efficiency of larger size crystals that could become available in a near future.

In the present paper, we present a detailed study of the self-activity for a commercial 1″ × 1″ $LaBr_3$:Ce together with data on the efficiency for γ-ray detection. The efficiency was measured at around 1 MeV and simulated in the interval 0.5–15 MeV for different detector sizes.

2. The $LaBr_3$:Ce detector

The investigated $LaBr_3$:Ce detector is a commercially available 1″ × 1″ crystal coupled to an XP2060 photomultiplier. The used voltage divider, delivered together with the detector, is model AS20 having 490 V as recommended operational voltage. The working voltage has to be kept rather low because of the extremely high photon yield produced by the crystal and of the fast photon emission time (smaller than 100 ns), which could cause a saturation of either the phototube or of the following electronic chain. For this reason, we determined how the dynamic range in which there is linearity between the signal and the energy can vary as a function of the applied voltage. This was made using the ^{152}Eu and ^{60}Co sources and by changing the voltage from 330 to 525 V. The linearity is maintained up to 500 V and the saturation appears at higher values.

The detector anode signals were directly fed into a spectroscopy amplifier CAEN model N568B. The amplifier was modified to remove the differentiation and to have the maximum gain in the first stage of the amplification. A shaping time of 0.5 μs was used. In Fig. 1 the measured energy resolution is shown as a function of γ-ray energy from various γ sources between 100 keV and 1.5 MeV, together with the expected $E^{-1/2}$ behaviour [17] normalized at the value of 2.8% at 662 keV, as declared by the manufacturer. An alternative approach, using a Silena QDC 4418 in a CAMAC-ECL data acquisition system, has produced an energy resolution 20% worse than the one obtained with the CAEN amplifier. In Fig. 2, the spectrum of the ^{60}Co source measured with the $LaBr_3$:Ce crystal is shown and compared with two other spectra, one measured with a hexagonal crystal 2″ × 3″ of BaF_2 (from the HELENA multiplicity filter [18]) and the other measured with a 3″ × 3″ NaI detector. One can see that for the two γ-rays at 1173 and 1332 keV the energy resolution of

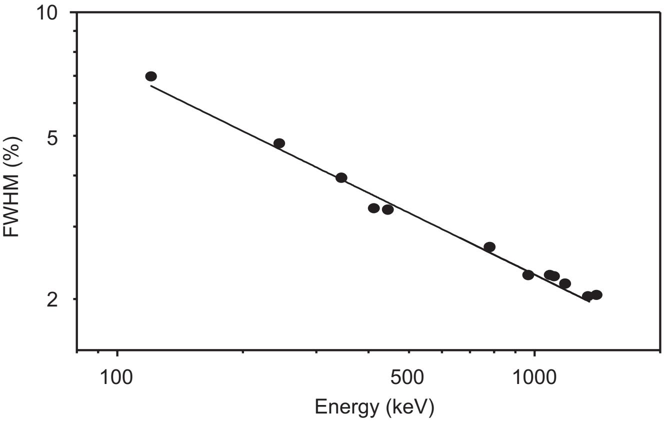

Fig. 1. Comparison of the measured energy resolution (filled points) with the expected $E^{-1/2}$ behaviour (full drawn line).

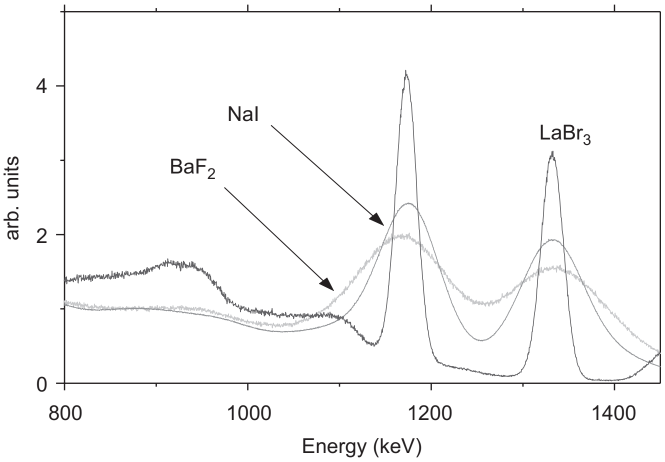

Fig. 2. Comparison of the ^{60}Co energy spectrum measured with the 1″ × 1″ $LaBr_3$ with those measured with a NaI and with a BaF_2 detector.

$LaBr_3$:Ce is at least two times better than that of the other two scintillators.

The timing properties of the $LaBr_3$:Ce detector were measured using a ^{60}Co source and a second identical $LaBr_3$:Ce crystal. A Tennelec TC454 constant fraction discriminator with a shaping delay of 12 ns was used and the thresholds were placed at the full energy peaks of the ^{60}Co. The counting rate was 2 kHz. A total time resolution of 320 ps was measured. The intrinsic time resolution of a single $LaBr_3$:Ce was therefore deduced to be approximately 230 ps.

3. Measurements of the internal activity of the $1'' \times 1''$ $LaBr_3$:Ce detector

The internal activity of the $LaCl_3$:Ce crystal (studied in Refs. [12–15]) is due to the presence of an unstable isotope, ^{138}La, and the contamination with the ^{227}Ac element, chemical homologue of lanthanum. For the $LaBr_3$:Ce, similar activities are expected [16].

The ^{138}La isotope is present in the natural lanthanum with an abundance of 0.09% and its lifetime is of the order of 10^{11} years. The self-activity due to its β decay is summarized in Table 1. The contamination due to the ^{227}Ac isotope produces also a β continuum up to ~1400 keV due to the β decay of ^{211}Pb and ^{207}Tl in the decay chain of this nucleus. There are also events due to α emission from ^{227}Th, ^{223}Ra, ^{219}Rn, ^{215}Po, and ^{211}Bi populated by the ^{227}Ac α-decay chain.

The self-activity in the $LaBr_3$:Ce crystal was measured both in singles and in coincidence/anticoincidence modes using the three different setups, named in the following as A, B and C:

- *Setup A*: Single events were measured shielding the detector with a ~10 cm thick lead layer and making use of the simple electronic chain described above.
- *Setup B*: The detector was placed inside a hollow BGO detector, detector usually used as an anti-Compton (AC) shield for HPGe detectors in γ-spectroscopy measurements. The front part of the shield was also closed with a BaF_2 scintillator to maximize the solid angle covered by active detectors. The Compton suppression technique is commonly used to clean γ spectra by rejecting events escaping the HPGe detector and requiring an anticoincidence condition. The thresholds of BaF_2 and BGO detectors were set just not to trigger on electronic noise. Coincidence (or anticoincidence) spectra were measured with the $LaBr_3$:Ce signals gated (or vetoed) by signals derived from the 'OR' between the signals of the surrounding BGO and BaF_2 detectors. In the present case, a background suppression factor (defined from the comparison of both spectra in the background region) of about 75% was measured for the γ-rays keV of the ^{60}Co source.
- *Setup C*: The detector was placed close to a HPGe detector with a thin beryllium window in order to make a coincidence measurement. This approach was also used in Ref. [12] for the $LaCl_3$:Ce crystal. In the present work, both detectors were shielded from external natural radioactivity using a layer of lead with a thickness of approximately 10 cm.

Table 1
Self-activity in $LaBr_3$:Ce crystals due to β decay

Isotope	Decay	E_{β^-} (keV)	I_e (%)	E_γ (keV)	I_γ (%)
^{138}La	β^-	252±12	34	789	34
	EC		66	1436	66
^{211}Pb	β^-	1378±8	100		
^{207}Tl	β^-	1423±5	100		

Data are taken from Ref. [20].

Data were collected in list mode using a VME data acquisition system including the CAEN ADC V879 and TDC V878 modules in a KMAX environment [19].

4. Results

In the single measurement with setup A, the known lines corresponding to the emission from the ^{138}La decay and from the α decays of the ^{227}Ac chain were clearly observed, and the rate of the detector self-activity was measured to be 0.85 cts/(s/cm^3) in the energy interval 70–5000 keV. The α activity was found to be responsible for approximately 10% of the counts. The measured spectrum is shown in Fig. 3. Note that the light yield produced by the interaction of α particles in the crystal is significantly lower than that produced from the γ-rays. The activity rate turned out to be significantly different from that reported in

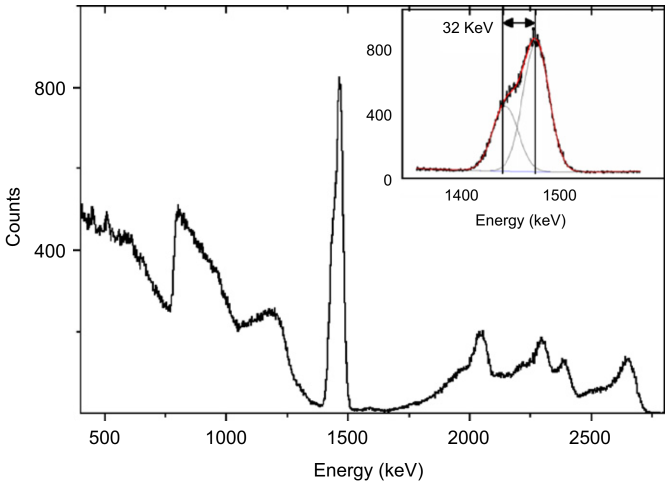

Fig. 3. The spectrum of the self-activity of the $LaBr_3$:Ce detector. The counts in the spectrum were binned at 2 keV/ch for an easier view. The events with energy smaller than 1.5 MeV are mainly due to the decay of ^{138}La while the structure between 1.5 and 3 MeV is produced by the decay chain of ^{227}Ac. In the inset, the peak structure centred around 1460 keV is shown together with the result of a fit procedure. There are two peaks centred at ~1440 and ~1470 keV.

Refs. [12–14]. Infact, in the most recent LaBr$_3$:Ce crystals, the contamination due to the presence of ^{227}Ac was reduced by almost two orders of magnitude in the manufacturing process [13]. Consequently, the ^{227}Ac activity is now comparable to that of ^{138}La. In addition, as the LaBr$_3$:Ce scintillator has an energy resolution which is approximately 25% better than that of LaCl$_3$:Ce, the peak at 1460 keV was found to have a structure. This peak consists of a superposition of γ-rays at 1461 keV from the natural environment radiation of ^{40}K and of γ-rays emitted in the electron capture of ^{138}La. The detailed structure of this peak has not been discussed in the existing works on LaBr$_3$:Ce although similar spectra for the self-activity were obtained [5,12]. The centroides of the two components of the structure are at ~1440 and ~1470 keV, respectively. The difference is approximately equal to the energy of the X-ray of Ba (32 keV) which is not always detected with the 1436 keV γ-ray of ^{138}Ba. The contribution of the ^{40}K line at 1460 keV has been estimated measuring the natural radioactivity with an HPGe detector for the same time interval in the same setup. It turned out that the decay from ^{40}K contributes for less than 15% to the counts in the peak.

In the setup B, the anticoincidence mode was used to clean the spectrum by rejecting events escaping the detector and retaining only singles events. On the other hand, by requiring a coincidence with the active shield, singles events, like the α decay to the daughter nucleus ground state, were rejected. Fig. 4 shows the comparison between the spectra obtained in coincidence and anticoincidence mode. In the anticoincidence spectrum, the structure superimposed over the β continuum, observed in the 800–1000 keV energy range is produced by the sum of the 789 γ-ray and of the associated continuum β^- decay of ^{138}La. At higher energy, between 1600 and 2800 keV, one can observe a more complex structure which is due to the α emission from ^{227}Th, ^{223}Ra, ^{219}Rn, ^{215}Po, and ^{211}Bi populated by the ^{227}Ac α decay chain.

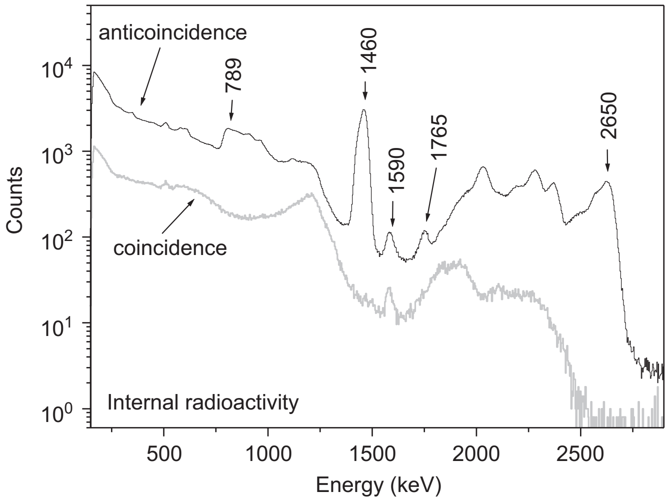

Fig. 4. Self-activity spectra of LaBr$_3$:Ce measured in coincidence (grey line) and anticoincidence (black line) with an active ~4π shield consisting of a BaF$_2$ detector and a BGO active anti-Compton shield. The spectra are normalized on the acquisition time.

In the coincidence spectrum, all peaks consisting of single transitions which deposit the full energy inside the crystal disappear. This is the case of the 1460 keV double peak consisting mostly of the 1436 keV transition of ^{138}Ba coming from the EC of ^{138}La, eventually summed to the Ba X-ray, and partly the 1460 keV transition from ^{40}K. Note that the threshold of LaBr$_3$:Ce is set at ~50 keV, higher than the ^{128}Ba X-ray energy. For the same reason the structure associated to the β^- decay of ^{138}La, from 789 to ~1000 keV, disappears. The peak observed at about 1590 keV corresponds to the second escape peak of the 2615 keV γ-ray coming from the natural environment. The first escape and the full energy peaks are masked by the α emission in LaBr$_3$:Ce. Only the Compton edge of the main peaks at 1460 keV and the second escape peak of the 2615 keV transition remain in the coincidence spectrum as they correspond to γ-ray scattering from LaBr$_3$:Ce to the AC shield or vice versa. In the coincidence spectrum the structure associated to the ^{227}Ac α decay chain is lower in excitation energy by few hundreds keV. Infact, when the parent nucleus decays through α emission directly to the ground state of the daughter nucleus, no γ-ray is emitted and the event is rejected in the coincidence mode. In particular, the structure at ~2650 keV, which completely disappears in the coincidence mode, corresponds to the 7386 keV α particles emitted from ^{215}Po that can only decay to the ^{211}Pb ground state. The structure observed in the coincidence spectrum corresponds to α decays to excited states, in such decays the energy of the α particle is smaller than that of the direct decay to the ground state.

A more detailed analysis of the α emission was obtained with the measurements with setup C. Fig. 5 shows a matrix

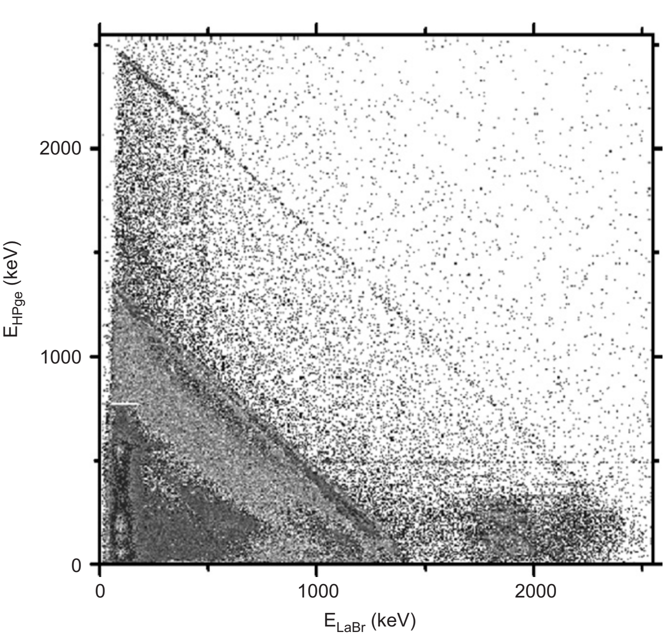

Fig. 5. The matrix of coincidence events measured with the LaBr$_3$:Ce (x-axis) and with the HPGe (y-axis) detectors.

containing coincidence events obtained with several weeks of data taking. The energies measured in coincidence with the $LaBr_3$:Ce and HPGe detectors are given in the x and y axes, respectively. The horizontal (vertical) lines in Fig. 5 correspond to γ-rays which have deposited all their energy in HPGe ($LaBr_3$:Ce) in coincidence with radiation in $LaBr_3$:Ce (HPGe), while the diagonal lines at 45°, namely $E_{\mathrm{HPGe}} + E_{\mathrm{LaBr_3}} = \text{constant}$, are associated to single photons which enter in one detector and then scatter out and are fully absorbed in the second detector. This is, for example, the case of γ-rays from ^{40}K at 1461 keV. Consequently, these lines at 45° constitute an unwanted source of background. The low energy γ-rays detected in the HPGe are in coincidence with β and α decays in the $LaBr_3$:Ce, the first being at low energy (below 1500 keV) and the second at higher energy.

Fig. 6 shows the spectrum of the electrons from the β^- decay due to the self-activity of the $LaBr_3$:Ce detector. These electrons were measured in coincidence with the 789 keV γ-ray transitions of ^{138}Ce detected in the HPGe detector. The Q-value of the β^- decay is 1044 keV. It is possible to note that, in contrast with what observed for $LaCl_3$:Ce [12], the light response of this scintillator to electrons does not seem to correspond to light production higher than that of γ-rays. In fact, the measured energy spectrum of the β particles, calibrated with γ-rays, dies at ≈250 keV, and this value is very close to the kinematical maximum energy of the β particle emitted by ^{138}Ce. The projection of the matrix of Fig. 5 on the HPGe axis for the events corresponding to the 'α' region in $LaBr_3$:Ce is shown in Fig. 7. The α-decay along the ^{227}Ac decay chain is in some cases followed by the de-excitation of the daughter nucleus through γ emission. The γ peaks corresponding to the various mother nuclei are indicated with different symbols.

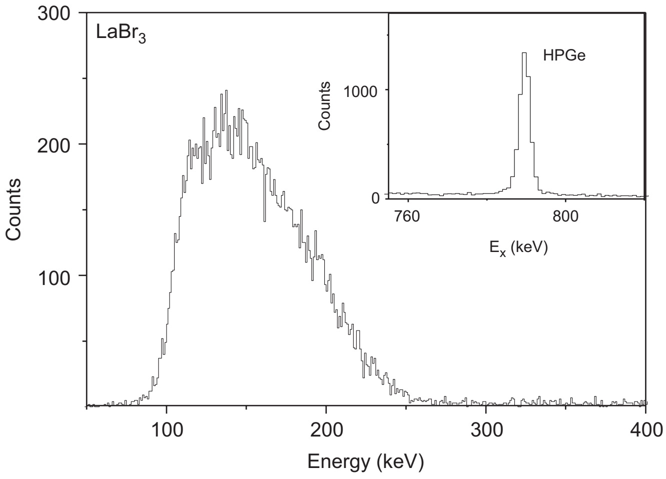

Fig. 6. Spectrum of the electrons from the self-activity of the $LaBr_3$:Ce detector measured in coincidence with the 789 keV γ-ray transitions in ^{138}Ce detected in the HPGe detector. The inset shows the peak at 789 keV.

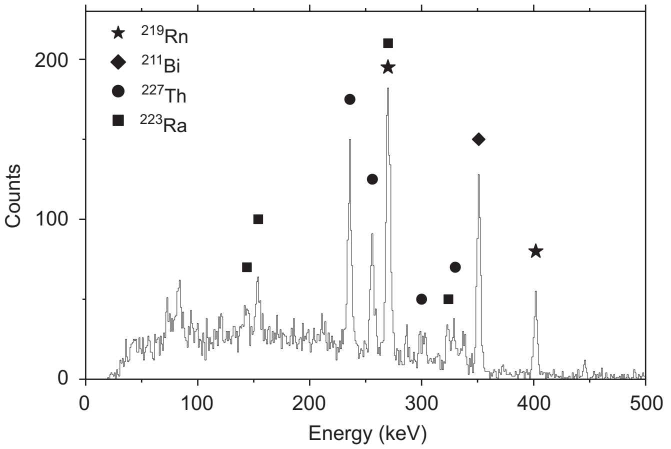

Fig. 7. The projection of the matrix of Fig. 5 on the HPGe axis. Only the region relative to the α decay ($1500\,\mathrm{keV} < E_{\mathrm{LaBr}} < 3000\,\mathrm{keV}$) has been selected. The different peaks are identified as given in the legend.

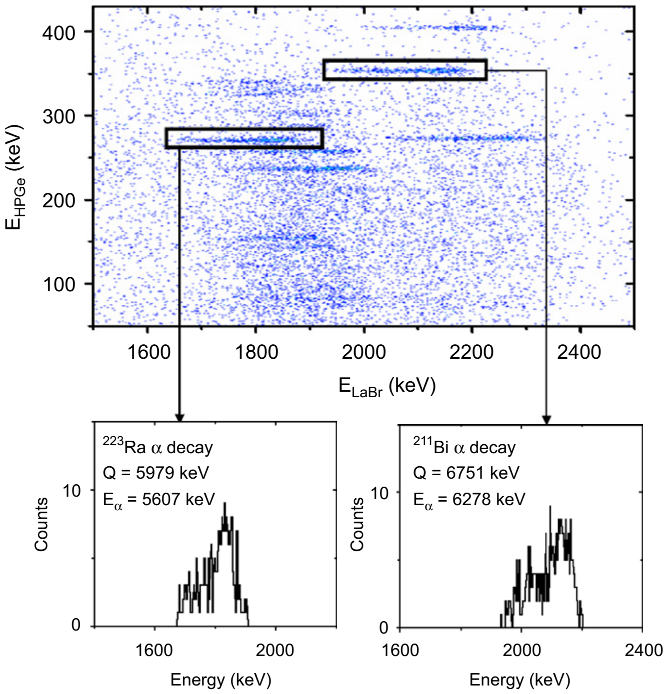

Fig. 8. The HPGe–$LaBr_3$:Ce coincident matrix expanded in the region of the α decay is given in the top panel. The α-particle spectrum measured in coincidence with the 269 keV transition of ^{223}Ra is in the bottom left panel while that in coincidence with and the 351 keV transition of ^{211}Bi decay is in the bottom right panel.

In Fig. 8, the α–γ region of the coincidence matrix is displayed together with the α particles spectra measured in coincidence with the 315 and 269 keV transitions in the ^{211}Bi and ^{223}Ra decays, respectively. The low energy tails appearing in the α peaks could be due to the energy deposited by the slow moving heavy recoiling nucleus (in different charge states) and to the quenching of the associated light yield.

In order to evaluate quantitatively the fraction of the radioactive elements present inside the $LaBr_3$:Ce crystal, the intensities of the α peaks, measured in coincidence with γ-rays, were obtained and these are listed in Table 2 in

Table 2
The comparison between the measured relative branch of α decay with that expected assuming secular equilibrium

Isotope	Q (keV)	E_α (keV)	E_γ (keV)	Absolute branch (%)	Relative branch (%)	Measured branch (%)
^{227}Th	6146	5756	256	7.0 ± 0.4	54 ± 3	66 ± 9
	6146	5756	236	12.3 ± 0.9	98 ± 7	118 ± 12
^{223}Ra	5979	5716	144	3.2 ± 0.1	25 ± 1	24 ± 11
			154	5.6 ± 0.1	43 ± 1	37 ± 9
		5607	269	13.7 ± 0.3	106 ± 2	106 ± 10
		5540	324	3.9 ± 0.1	30 ± 1	26 ± 8
			338	2.8 ± 0.1	22 ± 1	27 ± 8
^{219}Rn	6946	6553	271	10.8 ± 0.3	84 ± 2	89 ± 9
	6946	6425	402	6.4 ± 0.2	50 ± 2	47 ± 8
^{211}Bi	6751	6278	351	12.9 ± 0.1	100 ± 1	100

Note: Only the α particles in coincidence with γ-rays with absolute branch larger than 2% were selected. In the first column the mother nucleus is given. The Q-value (in keV), the energy of the emitted α particles (in keV) and the coincident γ-rays (in keV) are given in columns 2–4. The absolute branch for γ-ray emission, the previously known and the presently measured branches relative to that of ^{211}Bi are given in the last three columns, respectively. All known values are from Ref. [20]. The measured branches were normalized to the 351 keV line. The errors given for the presently measured branches include the statistical error of the measured 351 keV line.

comparison with the secular equilibrium expectations. In particular, in the first column the radioactive mother isotopes are indicated. The Q values, the energies of the α particles, of the coincident γ-rays, and the absolute α–γ-ray branches are given in columns 2–5, respectively. The expected α–γ-ray branches normalized to the ^{211}Bi α–γ decay and the corresponding measured values are listed in columns 6 and 7. In the evaluation of the intensities, the HPGe efficiency was taken into account. The given errors are of statistical nature only, which were estimated from the square root of counts in the gated α spectra.

As already mentioned, there is a difference in the scintillation light yield in LaBr$_3$:Ce produced by the interaction of γ-rays and of α particles of the same energy. A conversion factor can be deduced to express the α energy in equivalent γ-ray energy providing the same pulse height. Since we use internal radioactivity, one has to take into account also the energy deposited by the recoiling nuclei emitting the α particles. We have therefore extracted the conversion factor for this LaBr$_3$:Ce by fitting with a straight line the data providing the relation between the calculated and measured α energy. To measure the α energy we used the energy calibration for γ-rays, namely that obtained using known γ-ray energies from radioactive sources. The linear correlation of the data, in this energy range, is given by $E_\alpha = m \times E_\gamma + q$, with $m = 2.36$ ($\sigma_m = 0.06$), $q = 1.35$ MeV ($\sigma_q = 0.15$), confirmed by a correlation factor of $R = 0.9981$. In LaCl$_3$ the value of m was found to be 2.28 [12] or 2.16 [13]. For α particles the light yield is always more than a factor of 2 smaller than that of γ-rays of the same energy due to the quenching effect caused by their higher ionization density. With this conversion the energy resolution for α particles is ≈240 keV. The present results are shown in Fig. 9.

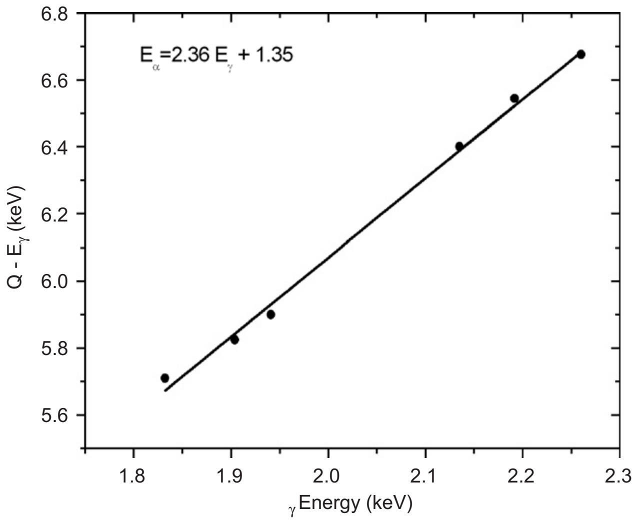

Fig. 9. The calculated α energy versus its corresponding measured value expressed in γ-ray energy equivalent (namely using the γ-ray energy calibration). The smaller light yield for α particles reflects the quenching due to their higher ionization density.

5. The efficiency of the LaBr$_3$:Ce crystal

The investigated detector, with its rather small volume 1″ × 1″ is characterized by a relative efficiency at the 1.173 MeV of 7.3 ± 1%, as presently measured with the ^{60}Co source. Consequently, it is not of ideal use in γ spectroscopy when the energies of interest are well over 1 MeV and extend up to 15–20 MeV. Recently, 3″ × 3″ LaBr$_3$:Ce detectors became commercially available and, hopefully, in the near future even larger crystals might be produced. It is therefore interesting to compare the expected performances in terms of full-energy peak efficiency of a large volume LaBr$_3$:Ce detector with the other detectors typically used in γ spectroscopy, namely a

3″ × 3″ cylindrical HPGe crystal (the typical size of detectors used in arrays like AGATA [21], EUROBALL [22–24] or GAMMASPHERE [25]) and a 6″ × 7″ tapered BaF_2 detector. Crystals of this size constitute the HECTOR array [26] which is used to measure γ-rays with energies between 5 and 25 MeV.

Detector arrays of HPGe and BaF_2 crystals are presently used in several laboratories and therefore the comparison between their efficiencies with that of $LaBr_3$:Ce of similar sizes (although not yet available) is important for the design of the forthcoming generation of gamma detection arrays. This comparison can be made by simulating the detector response as a function of γ-ray energy.

Simulations of the detector response to γ-rays were made using the GEANT4 [27] libraries. In the simulations the front surface of the crystal was uniformly hit by γ emitted by a point-like source placed at a distance of 30 cm. We simulated only interactions in the crystal and thus the crystal housing, the reflector or any kind of absorbers were not considered. In Fig. 10, the relative efficiencies of $LaBr_3$:Ce crystals of different sizes are plotted as a function of the γ-ray energy. For the 1″ × 1″ case, the simulations were compared to the experimental data obtained with a calibrated ^{60}Co source. For a fixed energy of the γ-rays the relative efficiency scales almost linearly with the size of the crystals, and a good efficiency is obtained for high energy γ-rays already for a 3″ × 3″ $LaBr_3$:Ce detector.

A direct comparison of the relative efficiency of two different size $LaBr_3$:Ce detectors with that of existing HPGe and BaF_2 detectors is shown in Fig. 11. In particular, a 3″ × 3″ HPGe and a 6″ × 7″ BaF_2 crystal (from HECTOR) are compared with $LaBr_3$:Ce crystals of the same sizes. The efficiency of the $LaBr_3$:Ce is found to be 30–50% larger than that of a HPGe, while it is comparable that of BaF_2 crystals.

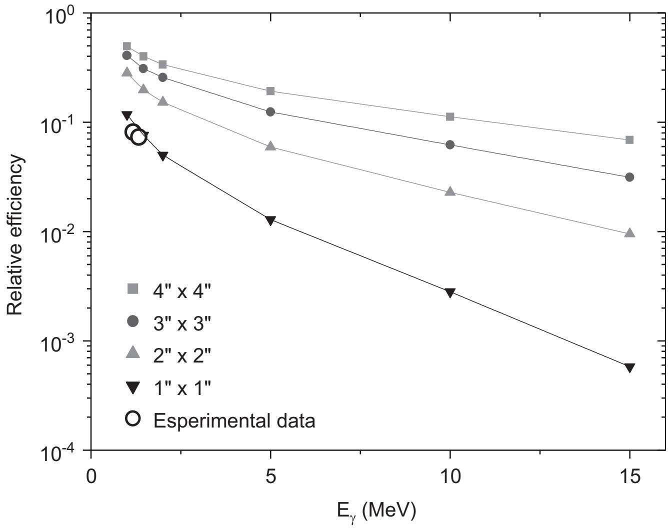

Fig. 10. The simulated (see text) relative efficiencies of cylindrical $LaBr_3$:Ce detectors of different sizes (in the legend) are plotted as a function of the energy of the incident γ-rays. The measured efficiencies at 1.173 and 1.332 MeV are shown by empty circles.

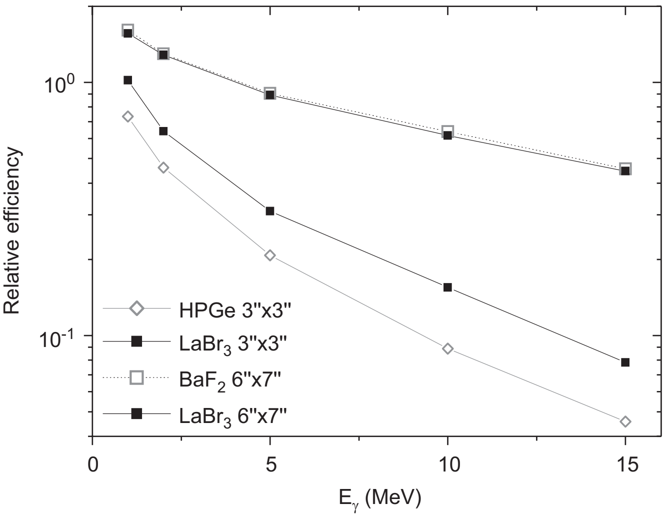

Fig. 11. The simulated relative efficiency of a 3″ × 3″ HPGe and a of tapered cylindrical 6″ × 7″ BaF_2 detector compared with that of $LaBr_3$:Ce crystals of the same size.

The results of the simulation reported in Figs. 10 and 11 indicate that 3″ × 3″ $LaBr_3$:Ce detectors can effectively compete with HPGe in an energy range between 1 and 10 MeV. In fact, compared to HPGe the $LaBr_3$:Ce has a higher efficiency, a similar spectral line-shape, good energy resolution to easily separate the full energy peak from the first and second escape and much superior timing properties. In addition, it does not need any cooling and consequently, it is much easier to handle. Compared to BaF_2 detectors, $LaBr_3$:Ce crystals show similar efficiency, as expected because of their similar effective charge and mass, but they have a much better energy resolution (see Fig. 2). It would be therefore very promising to develop the technology to grow large size $LaBr_3$:Ce crystals.

6. Conclusions

The properties of a cylindrical 1″ × 1″ $LaBr_3$:Ce scintillator (Brillance 380) were investigated focussing on the study of the self-activity and on the efficiency for the detection of γ-rays. The detailed study of the self-activity of the crystal was performed by measuring signals from the $LaBr_3$:Ce detector using three different setups: in singles, in coincidence/anticoincidence with an active AC shield surrounding the detector, and in coincidence with a high resolution HPGe detector. As already observed [16], we found that the β decay is responsible for the low energy background radiation and of two γ transitions at 789 and 1436 keV while the α decay gives rise to a "bump" between 1.6 and 2.4 MeV. Contrary to what previously reported [12], the β response of this scintillator seems to be similar to the γ response. The energy resolution for α particles with

5–7 MeV was measured to be ~240 keV. The conversion factor between γ-rays and α particles for the light yield corresponding to the same energy deposited was found to be ≈2.4. Therefore, the presence of self-activity in the $LaBr_3$:Ce scintillator detectors allows to use the internal light due to the interaction of the decay products as a monitor for the gain stability. The measured activity and the corresponding intensities of the measured transitions were understood in terms of the secular equilibration law.

The efficiency of the present detector and of larger volume detectors was investigated by performing simulations for γ-rays up to 15 MeV. It was found that a $3'' \times 3''$ crystal would have an efficiency larger than that of a HPGe of the same volume in the whole interval 1–15 MeV while its energy resolutions at 1.3 MeV is ≈25 keV and hence is much worse than for HPGe. However, energy resolutions of this type can be adequate in particular situations requiring not very high resolution but rather high efficiency. Moreover, the very good timing properties could easily allow time measurements (e.g. for isomer studies in the picosecond region) and to discriminate neutrons using time of flight techniques. If larger volume detectors (at least $3'' \times 3''$) will become available they will be surely of potential use in γ-spectroscopy studies because of their good energy and time resolution.

Acknowledgements

The authors would like to thank the Legnaro nuclear spectroscopy group and in particular G. De Angelis for allowing the use of the second $LaBr_3$:Ce detector employed in the time measurements.

References

[1] C.M. Rosza et al., Performance summary: Brillance scintillators $LaCl_3$ and $LaBr_3$, Saint Gobain crystals, available at ⟨www.detectors.saint-gobain.com⟩.

[2] E.V.D. van Loef, et al., Nucl. Instr. and Meth. A 486 (2002) 254.

[3] A. Iltis, et al., Nucl. Instr. and Meth. A 563 (2006) 359 and references therein.

[4] J. Glodo, et al., IEEE Trans. Nucl. Sci. NS-52 (2005) 1805.

[5] F. Quarati, et al., Nucl. Instr. and Meth. A 574 (2007) 115.

[6] W.W. Moses, Nucl. Instr. and Meth. A 487 (2002) 123.

[7] K.S. Shah, et al., IEEE Trans. Nucl. Sci. NS-51 (2004) 2395.

[8] H.J. Wollersheim, et al., Nucl. Instr. and Meth. A 537 (2005) 637.

[9] F. Camera, Ph.D. Thesis, University of Milano, Department of Physics, Italy, 1992.

[10] F. Camera, et al., Nucl. Phys. A 572 (1994) 401.

[11] A. Maj, et al., Nucl. Phys. A 571 (1994) 185.

[12] B.D. Milbrath, et al., Nucl. Instr. and Meth. A 547 (2005) 504.

[13] J.K. Hartwell, R.J. Gehrke, Appl. Radiat. Isot. 63 (2005) 223.

[14] B.D. Milbrath, et al., IEEE Trans. Nucl. Sci. NS-53 (2006) 3031.

[15] B.D. Milbrath et al., PNNL-15453.

[16] W.J. Kerman, IEEE Trans. Nucl. Sci. NS-53 (2006) 395.

[17] G.F. Knoll, Radiation Detection and Measurement, Wiley, 1999.

[18] M. Mattiuzzi, et al., Nucl. Phys. A 612 (1997) 262;
M. Mattiuzzi, Graduation Thesis, University of Milano, Department of Physics Italy.

[19] R. Bassini, et al., IEEE Trans. Nucl. Sci. NS-45 (1998) 858.

[20] R.B. Firestone, L.P. Ekstrom, Table of radioactive isotopes, ⟨http://ie.lbl.gov/toi/⟩.

[21] D. Bazzacco, Nucl. Phys. A 746 (2004) 248C.

[22] J. Simpson, Z. Phys. A 358 (1997) 139.

[23] B. Million, et al., Nucl. Instr. and Meth. A 452 (2000) 422.

[24] F. Camera, et al., Nucl. Instr. and Meth. A 351 (1994) 401.

[25] M.A. Deleplanque, R.M. Diamonds (Eds.), Gammasphere proposal, Lawrence Berkeley Laboratory Report 5202, 1988.

[26] O. Wieland, et al., Phys. Rev. Lett. 97 (2006) 012501.

[27] GEANT4 detector description and simulation tool, CERN, Geneva, Switzerland, 1993 and ⟨www.info.cern.ch/asd/geant⟩.